J. Phys. D: Appl. Phys. **42** (2009) 095416 (9pp) doi:10.1088/0022-3727/42/9/095416

Thermal transport in Si/Ge nanocomposites

Xiaopeng Huang[1,2,3], **Xiulan Huai**[1], **Shiqiang Liang**[1] **and Xinwei Wang**[3,4]

[1] Institute of Engineering Thermophysics, Chinese Academy of Science, 100080 Beijing, People's Republic of China
[2] Graduate School of the Chinese Academy of Science, 100080 Beijing, People's Republic of China
[3] Department of Mechanical Engineering, Iowa State University, 2010 Black Engineering Building, 50011 Ames, IA, USA

E-mail: xwang3@iastate.edu

Received 25 November 2008, in final form 13 March 2009
Published 16 April 2009
Online at stacks.iop.org/JPhysD/42/095416

Abstract
In this paper, a systematic study is carried out to investigate the thermal transport in Si/Ge nanocomposites by using molecular dynamics simulation. Emphasis is placed on the effect of nanowire size, heat flux, Si/Ge interface, atomic ratio and defects (voids). The results show that the thermal conductivity of nanowire composites is much lower than that of alloy, which accounts mainly for ZT enhancement and owes a great deal to the effect of interface thermal resistance. A 'reflecting effect' in temperature distribution is observed at the Si/Ge interface, which is largely due to the lack of right quantum temperature correction in the region adjacent to the interface. The thermal conductivity of the nanocomposite is found to have weak dependence on the bulk temperature (200–900 K) and the heat flux in the range (0.5–3.5) $\times 10^{10}$ W m^{-2}. Simulation results reveal that for a constant Si wire dimension, the thermal conductivity of the $Si_{1-x}Ge_x$ nanocomposites increases with x. Our study on the influence of the defects (voids) has the same order of relative thermal conductivity reduction with increasing void density in comparison with the experimental data. Due to the small size (10 nm) of Si nanowires in our nanocomposites, the voids show less effect on thermal conductivity reduction in comparison with the experimental data with 100 nm Si wires.

(Some figures in this article are in colour only in the electronic version)

1. Introduction

The efficiency and energy density of thermoelectric materials and devices are determined by the figure of merit $ZT = S^2\sigma T/k$, where S is the thermopower or the Seebeck coefficient, σ is the electrical conductivity, k the thermal conductivity and T the absolute temperature. The best thermoelectric materials are described as 'phonon-glass electron-crystal' (PGEC). This means that materials with low lattice thermal conductivity such as glass and high electrical conductivity as crystals are preferred [1]. Heavily doped semiconductors are on top of the list [2] for efficient thermoelectrical materials. In semiconductors, both electrons and phonons contribute to thermal conductivity while the phonons contribution is dominant. It has been a sound approach to reduce the phonon thermal conductivity of semiconductors in order to improve ZT. The enormous advance in nanoscience and nanotechnology has made it more feasible to design better thermoelectrical materials based on nanostructures including nanowire arrays, superlattices or quantum dot superlattices and nanotubes or nanocapsules [3–6]. Superlattices grown by thin film deposition techniques, however, are not suitable for large scale applications. The reduced thermal conductivity in superlattices is largely due to the sequential interface scattering of phonons rather than the coherent superposition of phonon waves [7, 8]. These lead to the idea of using nanocomposites as a potential economic alternative to superlattices in the search for high ZT thermoelectric materials [7]. Such nanocomposites can be fabricated by embedding nanoparticles or nanowires in a host matrix material, or mixing two different kinds of nanoparticles [8–10]. In practice, most crystalline materials

[4] Author to whom any correspondence should be addressed.

are not perfect. The regular pattern of atomic arrangement is interrupted by various types of crystal defects, including point defects, line defects, planar defects and bulk defects. These defects can strongly reduce the thermal conductivity of crystalline materials [11–14]. The synthesis process of nanocomposites usually will result in many defects (e.g. pores). Defects contribute much to phonon thermal conductivity reduction due to the enhancement of phonon scattering. However, little research has been reported about the defect effect on thermal conductivity reduction.

The molecular dynamics (MD) method has been applied to the investigation of nanoscale heat transfer for a long time. Stillinger and Weber [15] proposed a notable potential model to describe the interactions among Si atoms in solid or liquid phase. Lukes *et al* [16] used MD to investigate the thermal conductivity of solid thin films in the thickness direction. Chen's group simulated the thermal conductivity of Si crystals, Si nanowires and Si/Ge superlattice based on MD simulations [17–19]. Furthermore, the thermal properties of single or multi-wall carbon nanotubes have been investigated by using MD widely [20, 21]. The MD method is suitable for studying defects such as impurities, voids, pores and grain boundaries in materials [22–25]. The thermal properties of nanocomposites with and without defects, however, have rarely been studied by using MD simulation. Most of the previous studies on these materials are experimental work [26] or theoretical investigation using the double Gauss–Legender quadratures method [8] or the Monte Carlo (MC) method [9] to solve the phonon Boltzmann transport equation (BTE). Recently, a method called energy-conserving dissipative particle dynamics (eDPD) was introduced to simulate the heat conduction in nanocomposites [27]. In this method, a batch of molecules are treated as a nanoparticle embedded in a host matrix. The heat capacity of the particle and the particle–matrix interfacial thermal resistance are based on other work, and could not be directly calculated in eDPD. Additionally, strong phonon scattering within and around the nanoparticles can strongly reduce the thermal conductivity of particle and the matrix. Such effect is also difficult to predict in eDPD. The interfacial thermal resistance and phonon scattering effect is just what we want to study in this work. Therefore, the eDPD method is not suitable for our purpose.

In this paper, we use MD simulations to study the thermal transport in Si/Ge nanocomposites with and without voids, which are of great importance for developing high-efficiency thermoelectric materials. Emphasis is placed on how and to what extent the thermal conductivity of Si/Ge nanocomposites is affected by temperature, atomic percentage, heat flux, wire dimension and voids.

2. Theoretical model of simulation

2.1. Basis of MD simulation and thermal conductivity calculation

From the statistical physics point of view, there are two MD methods for studying the thermal conductivity of materials: equilibrium molecular dynamics (EMD) and nonequilibrium molecular dynamics (NEMD). The thermal conductivity in a homogeneous material can be calculated using either EMD with the Green–Kubo formula [17–19, 28] or NEMD simulation [29, 30]. The main challenge in performing NEMD simulations is to choose a suitable thickness or the total number of atoms in sample sections in order to establish local thermal equilibrium and calculate the local temperature. In quantum mechanics systems, thermal equilibrium is established by the anharmonic coupling of the vibrational normal modes, or phonon–phonon scattering. The key relevant quantity is the total number of phonon–phonon scattering events per section during the entire simulation run. It is determined by the relation [30]

$$N_{\mathrm{scat}} = 3N_{\mathrm{s}}\frac{\tau_{\mathrm{sim}}}{\tau_{\mathrm{ph}}}, \tag{1}$$

where N_{scat} is the total number of scattering events during the total simulation time τ_{sim} in a section containing N_{s} atoms and τ_{ph} is the average interval between the scattering events of each phonon. Previous work found that ~30 atoms in one section are adequate for equilibrium [30]. It is also found that in our simulations the local thermal equilibrium is indeed established in relatively thin sections in which the velocity distribution of atoms follows the Maxwell–Boltzmann distribution.

In the past, periodic boundary conditions used in most equilibrium MD simulations were not conveniently matched in NEMD. After years of work by Evans and Morris [31], Ciccotti and co-workers [32], Gillan [33], Ikeshoji and Hafskjold [29] and Miller-Plathe [34], several algorithms of periodic boundary conditions in a NEMD system have been developed. In this work, we use the algorithm developed by Ikeshoji and Hafskjold. In this method, a fixed amount of energy is added into a hot slab by scaling each hot atom's thermal movement by the same factor R while keeping the momentum conserved. The same amount of energy is removed from a cold slab by using the similar procedure. This algorithm has been used in the work by Jund and Jullien [35] and Lukes *et al* [16].

In this work, the Stillinger–Weber (SW) potential [15] is used for simulating Si and Ge. For Si, we choose the same values for all parameters in reference [15]. For Ge, we employ the parameters proposed by Ding and Anderson [36]. As for the Si–Ge interaction, we follow the method of Volz *et al* [28] by using the arithmetic mean coefficients.

In MD simulations, the temperature can be easily calculated from the time average kinetic energy of atoms in the sample section within the simulation time using the energy equipartition theorem:

$$\frac{1}{2}\sum_{i=1}^{N_{\mathrm{s}}} m\langle v_i^2\rangle = \frac{3}{2}N_{\mathrm{s}}k_{\mathrm{B}}T, \tag{2}$$

where $\langle\rangle$ denotes averaging over the total simulation time, and k_{B} is the Boltzmann's constant. The above equation is only valid at temperatures much higher than the Debye temperature. In this work, the thermal conductivity of Si/Ge nanocomposites at temperatures of 200–900 K is investigated. On the other hand, the Debye temperature (Θ_{D}) of Si and Ge is 645 K and 374 K, respectively [37]. In this work, the quantum definition

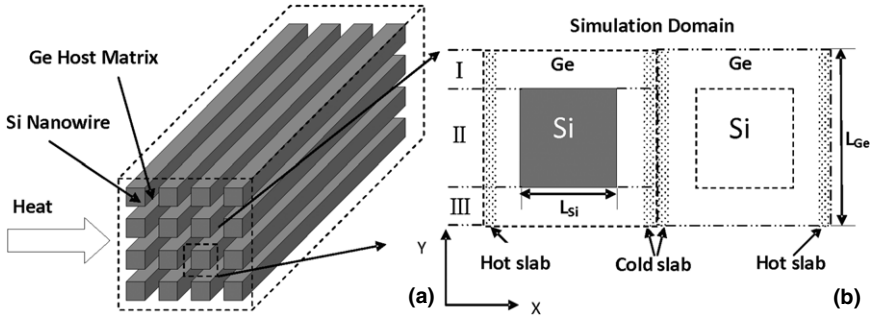

Figure 1. (*a*) Heat flux across a periodic 2D composite with Si nanowires embedded in Ge host matrix [8], (*b*) the unit cell of NEMD to show the location of the hot slab (energy supplied) and cold slab (energy withdrawn).

of the temperature in the Debye model is used, which could be calculated from the following equation [30]:

$$\frac{3}{2}N_s k_B T_{NEMD} = \frac{1}{2}\int_0^{\omega_D} D(\omega)N(\omega, T)\hbar\omega \, d\omega, \qquad (3)$$

where $D = V\omega^2/(2\pi^2 v^3)$ is the Debye density of states, and $N = 1/(e^{\hbar\omega/k_B T} - 1)$ is the phonon occupation number given by the Bose–Einstein distribution corresponding to the local equilibrium temperature T (the quantized temperature), ω the phonon frequency, ω_D the Debye cutoff frequency, V the volume of lattice cell and v the group velocity. T_{NEMD} is the classic temperature in nonequilibrium MD programs which represents the average kinetic energy of atoms. By numerically integrating the right side of equation (3), a one-to-one correspondence between T_{NEMD}/Θ_D and T/Θ_D can be obtained. Then the quantized temperature T could be calculated.

The thermal conductivity k is defined by the Fourier's law $J = -k\nabla T$, where J is the heat flux. Our work focuses on the thermal transport in nanowire-embedded composites for the case where the heat flow direction is perpendicular to the wire axis as shown in figure 1. Yang and Chen [8] have investigated the same problem by solving the phonon BTE using the double Gauss–Legendre quadratures method. Their results are taken as an important reference to evaluate whether our method is applicable to study the similar system. For the simplicity of programming, the local temperature is defined as the statistical temperature of a section, $T(x)$, where x denotes the midpoint of a section. The quantum correction will be done in the post-process. Then the effective thermal conductivity k can be calculated by,

$$k = -\frac{J}{\partial T/\partial x} = \frac{k_{NEMD}\partial T_{NEMD}/\partial x}{\partial T/\partial x} = \frac{J L_{Ge}}{T_{NEMD}(L_{Ge}) - T_{NEMD}(0)}\frac{\partial T_{NEMD}}{\partial T}, \qquad (4)$$

where $\partial T_{NEMD}/\partial T$ is obtained from equation (3). It is a function of T/Θ_D. Only the temperatures of Ge at the two ends are used in the calculation, so the Debye temperature Θ_D of Ge 374 K is chosen. It is convenient for experimentalists to calculate the thermal conductivity without knowing the temperature profile within the sample. The temperature profiles are studied in this work to get more understanding about the heat transport near the interface of the two components. According to equation (4), the temperatures of the hot and cold ends are specified, then the heat flux can be calculated, or a fixed heat flux is given, then the temperature gradient can be obtained. After several simulations, it is found that obtaining convergence of heat flux will take a longer time than obtaining stable temperature under a given heat flux. Thus, in this work the temperature profile is obtained under a specified heat flux. In our work, the (effective) thermal conductivity (k) is calculated by using the temperature at the hot (T_h) and cold ends (T_c), as well as the heat current (q) between them: $k = q\Delta x/[2(T_h - T_c)A]$, where A is the cross sectional area of the sample in the y–z plane and Δx is the distance between the heating and cooling slabs. The factor '2' accounts for the symmetrical effect of the computation.

2.2. Domain design for thermal conductivity calculation

The structure of Si/Ge nanocomposite, Si nanowires embedded in Ge host matrix, is illustrated in figure 1(*a*). The physical simulation domain is shown in figure 1(*b*). We divide the simulation domain into several sections along the x direction. The hot and cold slabs are the regions where we add and remove energy to establish the heat flux. Four atomic layers are specified in each hot and cold slab following the suggestion by Kotake and Wakuri [38]. Periodic boundary conditions are applied in all the three directions. Due to the two-dimensional feature of the system, one lattice constant thickness along the z direction is mainly used to reduce the computational time significantly. A case of double lattice constant thickness is also studied to observe the effect of the thickness. We have investigated different systems with the total atom number ranging from one thousand to ten thousand, in which we fix the Si wire dimension as $L_{Si} = 5$, 10, 20 and 50 nm. At these scales, we can compare our results with the experimental and numerical data of other groups. The characteristic length of Ge, L_{Ge}, is varied to investigate the thermal conductivity at different Si/Ge atom ratios. The region between the hot and cold slabs is divided into several sections under the principle of phonon scattering events that there are more than 30 atoms in every section. Thin sections are used near interfaces to obtain detailed effect of the interface and thick sections are used in other regions to reduce the statistical error, as will be shown in figure 2. In the y direction, the box is divided into three layers at the Si/Ge interface for studying the temperature profiles at

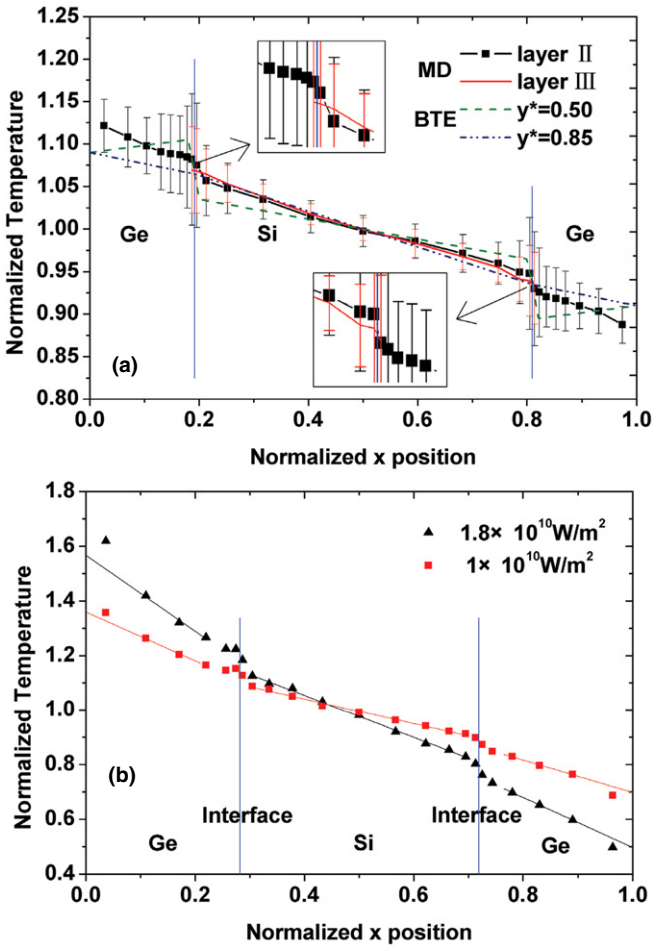

Figure 2. Nondimensional temperature T/T_{eq} profile in two composite structures: (*a*) $Si_{0.4}Ge_{0.6}$, $L_{Si} = 20$ nm, $T_{eq} = 600$ K, $J = 6 \times 10^9$ W m^{-2}, (*b*) $Si_{0.2}Ge_{0.8}$, $L_{Si} = 10$ nm, $T_{eq} = 200$ K, layer II. The temperature jumps at the interface are clearly shown in the inset in figure (*a*). The temperature shown in this figure does not include the quantum correction due to the fact that materials close to the Si/Ge interface do not have the Debye temperature of the bulk counterparts. The temperature profiles obtained by Yang and Chen solving phonon BTE using the numerical method [8] are also shown in the figure (*a*).

different y positions, as shown in figure 1(*b*). An optimal time step was found to be $\Delta t = 0.5$ fs. The velocity-Verlet [39] algorithm is used for integrating the motion equations of atoms.

In the calculation, first we put the Si and Ge atoms on their own lattice nodes with the lattice constants 5.431 Å and 5.658 Å, respectively. To obtain the appropriate initial structure of the material, we calculate 200 000 time steps of EMD at the desired temperature. Canonical ensemble NVT is used at this stage. A great number of simulations show that the sample sections need different time steps to reach steady state at different heat flux and different characteristic length. More time steps are needed for higher heat flux and larger scale systems. Therefore, the computation time of NEMD is varied under the guidance that the computation continues at least 300 000 time steps after the convergence of temperature gradient. Also in the simulation the temperature gradient/profile in the system is checked to make sure it will not change with time, which is an indication of the steady state. The total number of time steps of NEMD is from 500 000 to 2000 000. Microcanonical ensemble NVE is used at this stage. At final, the stable temperature profile is obtained by statistical averaging. Due to the symmetry of the simulation domain, the final temperature profile is given by averaging the temperatures in corresponding sections of two symmetrical slabs with respect to the central symmetrical line. The standard deviation from statistical averaging is used to calculate the uncertainty of the thermal conductivity by using the function of error propagation. The computation time of each case varies from a few hours to several days, depending on the total number of atoms considered.

3. Results and discussion

With respect to nanocomposites, the thermal transport regime in it is more complex than in bulk single crystals. There are more factors that could affect the thermal conductivity of nanocomposites. In this work, the effect of temperature, heat flux, atomic percentage, wire dimension and voids are considered.

3.1. Temperature profile

Figures 2(*a*) and (*b*) show the temperature profiles along the direction of heat flux (x direction) in two composites: (1) $Si_{0.4}Ge_{0.6}$, $L_{Si} = 20$ nm, $T_{eq} = 600$ K, (2) $Si_{0.2}Ge_{0.8}$, $L_{Si} = 10$ nm, $T_{eq} = 200$ K. The thickness of different systems is all one lattice constant unless other values are noticed. Similar temperature profiles are also obtained for the case of 450, 750 and 900 K and are not shown here. The x position is normalized with respect to the characteristic length L_{Ge}. The normalized temperature is calculated with respect to the equilibrium temperature T_{eq}. The temperature quantum correction is not considered in figure 2 due to the fact that materials close to the Si/Ge interface do not have the same Debye temperature as the bulk counterparts. The statistical error in figure 2 is obtained from the standard deviation from statistical averaging of the temperature at different time steps. The temperature in the case is recorded every 100 time steps. It is clearly shown in figures 2(*a*) and (*b*) that after a linear decrease an obvious upward deviation in temperature distribution occurs to the left side of the Si/Ge interface, then the temperature jumps down across the interface. This upward deviation is more like a 'reflecting effect' and the downward jumps are due to the Kapitza resistance [40, 41]. In layer III (pure Ge), the downward jumps at the interfaces are not sharp, but are still visible. It reveals that layer III is not thick enough to ignore the effect of the interface from the neighbouring regions. We do not do the quantum correction for the temperature distribution because we cannot just use the same Debye temperature everywhere for Si or Ge. The Debye model is a predigested model and the Debye temperature is used for bulk materials. However, when an interface exists, phonon scattering happens and the dispersion relation is not as the one in the bulk material. The influence of interface on dispersion relation is not clear so far, thus the quantum correction cannot

be exactly done. Actually, we have made an attempt to conduct quantum correction for Si and Ge part with $\Theta_D = 645$ K and 374 K, respectively. The result shows that for layer II the Si part temperature goes below that of Ge at the cold end, leading to a negative Kapitza resistance. If using the average Debye temperature of Si and Ge for materials in vicinity of the Si/Ge interface, the temperature distribution across the interface is smoother with a positive Kapitza resistance. Additionally, the 'reflecting effect' at the Si/Ge interface becomes weak. Thus, a more precise model considering the influence of interface on the dispersion relation is needed to do the quantum correction. From the above discussion, it can be inferred that the 'reflecting effect' is largely due to the lack of high-accuracy quantum correction.

A comparison is done between our temperature distribution with that obtained by Yang and Chen solving phonon BTE using the numerical method [8]. Their sketch curve is also shown in the figure. It needs to be pointed out that the temperature definition in this work is different from that in the work by Yang and Chen. The temperature defined in this work characterizes the average kinetic energy and the one defined by Yang and Chen characterizes the average energy density. Their results indicate that when the nanowire dimension is much smaller than the phonon mean free path (MFP), say $L_{Si} = 10$ nm, the temperature along the x direction can increase before entering the interface (meaning 'negative' thermal conductivity) and after exiting the interface, as shown in figure 2 in Ge. On the other hand, our results show that this abnormal temperature distribution disappears. The 'end effect' first presented by Maiti *et al* [30], which is a large temperature gradient at the two ends, also exists in our results. It is due to the enhanced scattering of phonons arising from energy fluctuation and local thermal nonequilibrium which is caused by maintaining constant heat flux. With the periodic boundary condition, this effect should not be counted in calculating the thermal conductivity. Therefore linear fits on the temperature at the sections away from the boundary are used, as shown in figure 2(*b*). The slope of the linear fitting lines at both ends for the three layers [I, II and III shown in figure 1(*b*)] are averaged for calculating the thermal conductivity.

A structure of $Si_{0.4}Ge_{0.6}$ with $L_{Si} = 20$ nm and double lattice constant thickness in the z direction is also investigated. It is found that the thermal conductivity of the nanocomposite with double lattice constant thickness is about 14% larger than the one with one lattice constant thickness. This result illustrates that the dimension used in the simulation also affects the phonon transport even under the periodic boundary condition. The larger the dimension in the simulation, the more the result represents the real situation. However, the computation time will increase significantly with the increasing computational domain. We find that the temperature profile shown in figure 2 does not change much for the case of two lattice constants in the z direction. The only difference is that when the material is thicker in the z direction, the statistical error is getting smaller due to the increased number of atoms for temperature calculation in each section.

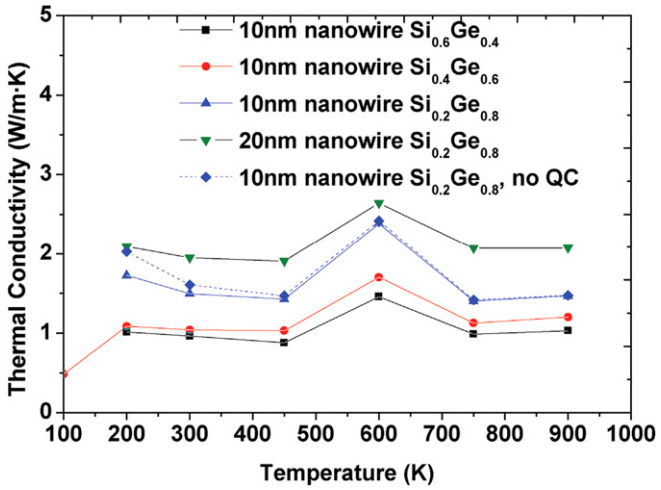

Figure 3. Thermal conductivity of different nanocomposite systems as a function of temperature. The thermal conductivity changes little with the temperature except in the vicinity of 600 K (QC: quantum correction).

3.2. *Effect of temperature*

Figure 3 shows the thermal conductivity of different Si/Ge nanocomposites at different temperatures. In the figure, the thermal conductivity is almost constant from 200 to 900 K except at 600 K. From all our simulations, it is found that at different system sizes the temperature of the sample reaches the steady state faster at 600 K than at other temperatures, and there is a smaller temperature difference between hot and cold slabs, leading to a larger thermal conductivity at 600 K. When the quantum correction is removed, the thermal conductivity abnormal behaviour around 600 K still exists. There is a difference (less than 15%) for the thermal conductivity with and without quantum correction below 300 K. However, when the temperature is at or above the Debye temperature, the quantum correction has a negligible effect on the thermal conductivity. Other numerical and experimental investigations on nanoparticle composites and superlattice systems also concluded that the thermal conductivity is weakly dependent on temperature from 200 to 1200 K [7, 10, 19, 42] and the thermal conductivity of superlattice at temperatures below 200 K is a little lower than that above 200 K [43, 44]. In this work, the range of temperature is 200–900 K for the conclusion that the thermal conductivity has a weak dependence on temperature. It is possible that the thermal conductivity could have a strong temperature dependence below 200 K and above 900 K, especially below 200 K. The heat capacity of Si and Ge decreases sharply at low temperature, and the phonon MFP is limited by the characteristic length. It is believed that the thermal conductivity of nanocomposites consisting of the two types of atoms will be heavily affected by temperature due to the proportional relation between heat capacity and thermal conductivity. For this reason, we did a case study at 100 K, in which the thermal conductivity is much lower than that at other temperatures as shown in figure 3. This agrees with the experimental conclusion that the thermal conductivity of superlattice at the temperature below 200 K is lower than that above 200 K [43, 44].

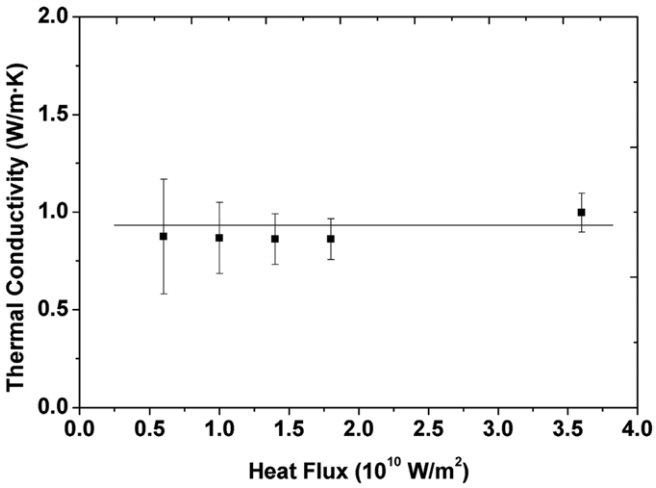

Figure 4. Thermal conductivity of $Si_{0.6}Ge_{0.4}$ composites as a function of heat flux for wire dimension of $L_{Si} = 10$ nm.

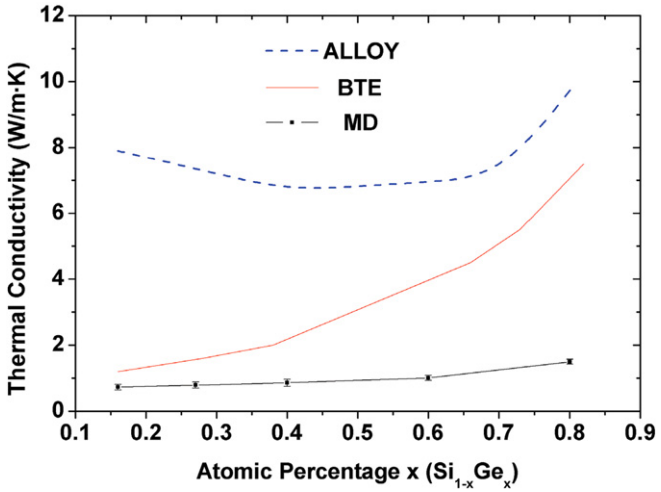

Figure 5. Thermal conductivity of $Si_{1-x}Ge_x$ composites obtained by the BTE [8] and MD method respectively as a function of atomic percentage x of Ge for wire dimension of $L_{Si} = 10$ nm.

3.3. Effect of heat flux

Recently Guo *et al* [45] established a theory of heat conduction based on the concept of heat-mass. It points out that in the wide case the heat conduction has not only temporal inertia effect of heat flux, but also spatial inertia effect of heat flux, and temporal and spatial inertia effect of temperature. In general, these effects could be negligible. However, when the temperature gradient and the heat flux are high enough, these effects become more important. This happens easily in nanoscale heat conduction. The change in distribution of phonon frequency may cause different phonon scatterings, which is highly related to the thermal conductivity. We choose a set of heat flux values to calculate the thermal conductivity of the nanocomposite in which the characteristic length of Si is 10 nm and the Ge atomic percentage is 40%, as shown in figure 4. The equilibrium temperature of the system is 300 K. Obviously, the thermal conductivity is almost constant under different heat flux values, so the heat flux in the magnitude of 10^{10} W m^{-2} does not influence the thermal conductivity so much.

3.4. Effect of atomic percentage

Figure 5 shows how the thermal conductivity of $Si_{1-x}Ge_x$ composites changes with the atomic percentage of Ge(x) for wire dimension of $L_{Si} = 10$ nm. The equilibrium temperature of the system is 300 K. The scale of Ge is changed in the simulation for different atomic percentages. It shows that for a constant Si wire dimension, the larger the atomic percentage of Ge, the larger the thermal conductivity of the Si/Ge nanocomposites. This is very different from macroscale composites, in which the effective thermal conductivity decreases with the increasing volumetric fraction of the lower thermal conductivity component. This can be explained by two reasons. One is the ballistic phonon transport in both the host material and the nanowires due to the characteristic length smaller than phonon MFP, which is called 'size effect'. The other is the interfacial thermal resistance between them, which just causes the temperature jump at the interface. With increasing atomic percentage of Ge for a constant size Si nanowire, the dimension of Ge increases and the interfaces per volume decrease, so the size effect and the interface effect on reducing thermal conductivity become weak and the thermal conductivity increases. Additionally, these two reasons could also explain why all the values of nanocomposites are much lower than the values of bulk alloy with the similar chemical composition. This exciting result illustrates that Si/Ge nanocomposites are indeed a cheap alternative to superlattice for high ZT. It should be noted that the thermal conductivity obtained by MD simulation is lower than that obtained by BTE numerical simulation. The possible reason for this difference is that in the z direction only one lattice constant is used in our model, which could give rise to more phonon scattering. The experimental data from Lee [46], which will be shown in section 3.6, indicates the MD results are still reasonable.

3.5. Effect of wire dimension

Figure 6 shows the thermal conductivity of $Si_{0.4}Ge_{0.6}$ composites at 300 K as a function of the Si wire dimension. It is shown clearly that at constant atomic percentage the thermal conductivity increases with the wire dimension, and among the selected dimensions this increase reveals a good linear relation. This linear relation has a good agreement with previous studies [8, 10, 16]. Through linear fitting of the data points, a correlation is given as below:

$$k = 0.6 + 0.032 L_{Si}, \tag{5}$$

where the unit of L_{Si} is nm and the unit of k is W m^{-1} K^{-1}. The increase in thermal conductivity with dimension is due to the fact that the phonon MFP will be less affected by the size and will be longer. Another reason is the number of interfaces per volume goes down when the wire dimension is getting larger. As a result, the phonon scattering decreases and the influence of interface thermal resistance becomes smaller. Considering that the thermal conductivity of composites will reach the alloy

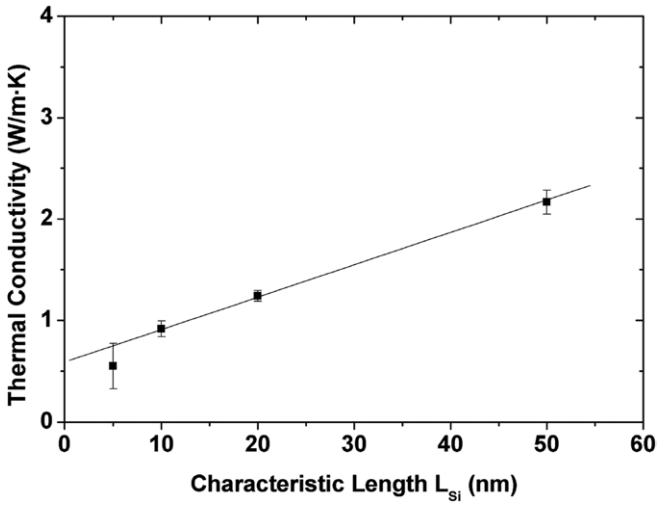

Figure 6. The thermal conductivity of $Si_{0.4}Ge_{0.6}$ composites at 300 K as a function of the Si wire dimension. The solid points are the results from MD simulation, and the solid line is the linear fitting of the results.

value with the same atom ratio when the Si nanowire goes to a large scale, the $k-L_{Si}$ correlation should deviate from linearity at large L_{Si}.

3.6. Effect of voids

A schematic of $Si_{0.4}Ge_{0.6}$ nanowire composites with 4.8% density voids is shown in figure 7(*a*). In practice, the composites are often obtained by hot pressing of two mixed components. This usually produces a lot of voids especially at the interface. Therefore, in the model the voids are placed at the Si/Ge interface. In our work, each void is smaller than 3 unit cells, so there is little surface effect for special treatments in the vicinity of the defects. In fact, we allow the defects to evolve in the simulation to stablize before applying the heating and cooling. The temperature profiles with different void densities are shown in figure 7(*b*). Obviously, the temperature jumps as well as interface thermal resistances at the interface increase with the void density, and the temperature difference between the hot slab and the cold slab also increases with the void density under the same heat flux. The existence of voids reduces the heat transfer and increases the interface thermal resistance, so the thermal conductivity is reduced. The thermal conductivity varies with the void density as shown in figure 8. The experiment data from Lee [46] shown in table 1, although for a different nanocomposites system, can be used for comparison. The experimental data indicate that the thermal conductivity of $Si_{0.8}Ge_{0.2}$ composites with 10% void density for 100 nm Si nanowire decreases by 61% with respect to that has 2% void. In our results, the corresponding decrease ratio is 34% for $Si_{0.4}Ge_{0.6}$ composites for 10 nm Si nanowire. It is less than the experiment value. The reason is that the voids in larger scale composites have a more significant effect in reducing the phonon MFP and enhancing the phone scattering. Obviously, the $Si_{0.8}Ge_{0.2}$ composites with 100 nm Si nanowire has longer phonon MFP than the $Si_{0.4}Ge_{0.6}$ composites of 10 nm Si nanowire if there are no

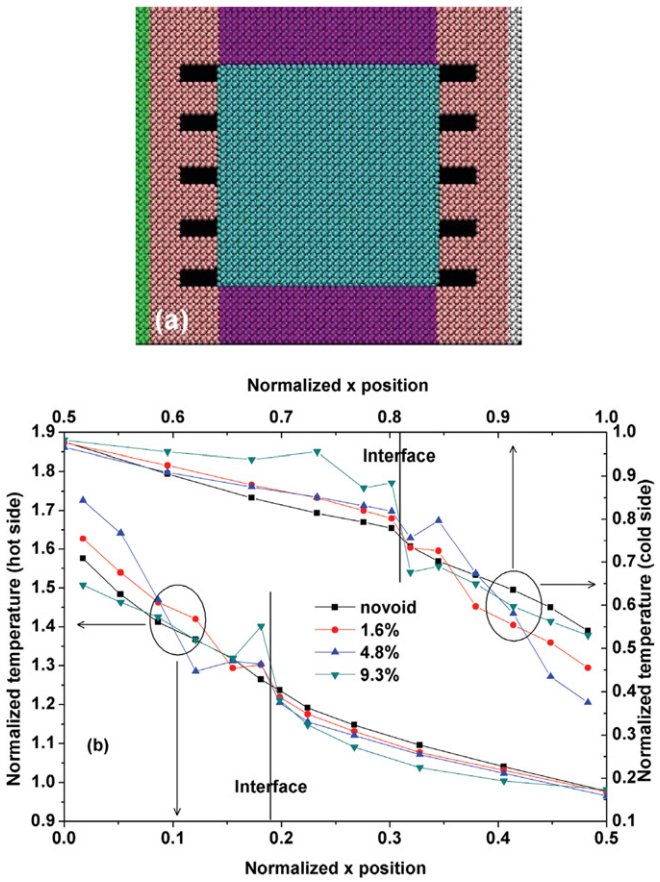

Figure 7. (*a*) A snapshot of the physical domain design. The black regions are the voids and (*b*) normalized temperature profile in layer II of $Si_{0.4}Ge_{0.6}$ nanowire composites with different void density for wire dimension of $L_{Si} = 10$ nm at the equilibrium temperature of 300 K. In the 9.3% case the heat flux is 1×10^{10} W m^{-2}, and in other cases the heat flux is 1.8×10^{10} W m^{-2}.

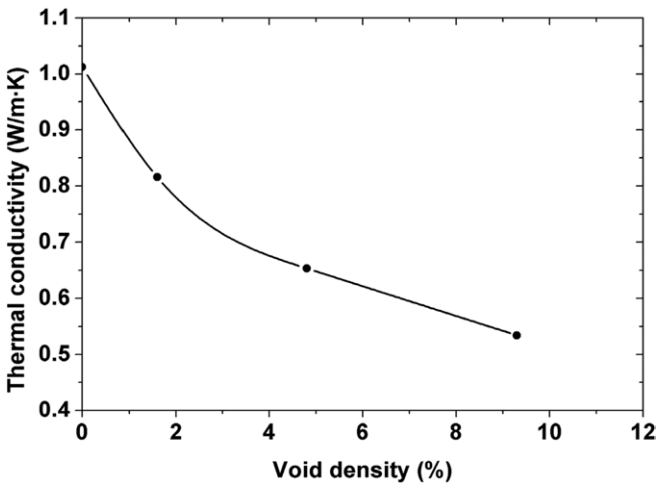

Figure 8. Thermal conductivity of $Si_{0.4}Ge_{0.6}$ nanowire composites varies with the void density for wire dimension of $L_{Si} = 10$ nm at the temperature of 300 K.

void in the systems. Voids will reduce the phonon MFP. The reduction is larger for longer phonon MFP. Therefore the reduction ratio of thermal conductivity of composites with thicker nanowires with respect to void density is larger than

Table 1. The thermal conductivity of nanocomposites with $L_{Si} = 100$ nm.

	$Si_{0.8}Ge_{0.2}$ void density: 2%	$Si_{0.8}Ge_{0.2}$ void density: 10%	$Si_{0.2}Ge_{0.8}$ void density: 17%
Thermal conductivity ($W\,m^{-1}\,K^{-1}$)	4.27	1.66	5.07

that consisting of thinner nanowires. A larger structure with $L_{Si} = 50$ nm for $Si_{0.8}Ge_{0.2}$ without void is also simulated in order to compare with experimental data as closely as possible. The thermal conductivity is $1.53\,W\,m^{-1}\,K^{-1}$, which is much smaller than the thermal conductivity of the experimental result for the case of $Si_{0.8}Ge_{0.2}$ with 2% voids and 100 nm diameter Si nanowires. It again indicates that the characteristic size of the Si nanowire has a significant effect on the thermal conductivity of the composite.

4. Conclusion

This work studied the thermal conductivity of two dimensional nanocomposites with Si nanowires embedded in a Ge host matrix using NEMD. The results showed that the thermal conductivity of nanowire composites can be much lower than that of the alloy, which can be explained by ballistic phonon transport and interface thermal resistance. The simulation also revealed a 'reflecting effect' for the temperature distribution close to the interface of the two components. This phenomenon is largely due to the lack of high-accuracy quantum correction of the temperature. It was found that the thermal conductivity of Si/Ge composite was weakly temperature dependent in the range of selected system sizes and temperatures (200–900 K). Our study indicated that for a constant Si wire dimension, the thermal conductivity of the Si/Ge nanocomposites increased with the atomic percentage of Ge, which is due to the decrease in the ratio of interfaces to volume. An attempt to study the influence of the voids on thermal conductivity showed that the thermal conductivity decreased with the void density. The relative thermal conductivity reduction versus the void density is lower than the experimental results for nanocomposites with $L_{Si} = 100$ nm because the voids in nanocomposites of thicker nanowires have a more significant effect in reducing the phonon MFP and enhancing phone scattering.

Acknowledgments

The authors gratefully acknowledge the support of the National Natural Science Foundation of China under Grant #50776087, the Chinese National Key Foundation Research Subject under Grant #2006AA05Z203. This work is also supported by Supercomputering Center, the Computer Network Information Center (CNIC), Chinese Academy of Sciences (CAS) and the Institute of Engineering Thermophysics, CAS. Partial support from the start-up fund of Iowa State University is gratefully acknowledged.

References

[1] Slack G A 1995 *CRC Handbook of Thermoelectrics* ed D M Rowe (Boca Raton, FL: CRC press)

[2] Ioffe A F 1957 *Semiconductor Thermoelements and Thermoelectric Cooling* (London: Infosearch Limited)

[3] Prieto A L, Sander M S, Martín-González M S, Gronsky R, Sands T and Stacy A M 2001 Electrodeposition of ordered Bi_2Te_3 nanowire arrays *J. Am. Chem. Soc.* **123** 7160–1

[4] Venkatasubramanian R, Siivola E, Colpitts T and O'Quinn B 2001 Thin-film thermoelectric devices with high room-temperature figures of merit *Nature* **413** 597–602

[5] Harman T C, Taylor P J, Walsh M P and LaForge B E 2002 Quantum dot superlattice thermoelectric materials and devices *Science* **297** 2229–32

[6] Ji X H, Zhao X B, Zhang Y H, Sun T, Ni H L and Lu B H 2004 Novel thermoelectric Bi_2Te_3 nanotubes and nanocapsules prepared by hydrothermal synthesis *23rd Int. Conf. on Thermoelectrics (Adelaide, Australia, 25–29 July 2004)*

[7] Yang R and Chen G 2005 Nanostructured thermoelectric materials: from superlattices to nanocomposites *Mater. Integr.* **18** 31–6

[8] Yang R and Chen G 2004 Thermal conductivity modeling of periodic two-dimensional nanocomposites *Phys. Rev.* B **69** 195316–25

[9] Jeng M-S, Yang R and Chen G 2005 Monte Carlo simulation of thermoelectric properties in nanocomposites *24th Int. Conf. on Thermoelectrics (Clemson University, South Carolina, USA, 19–23 June 2005)*

[10] Tian W and Yang R 2007 Thermal conductivity modeling of compacted nanowire composites *J. Appl. Phys.* **101** 054320–4

[11] Kitttel C 2005 *Introduction to Solid State Physics* (New York: Wiley)

[12] Dudkin V V, Gorodilov B Y, Krivchikov A I and Manzhelii V G 2000 Thermal conductivity of solid krypton with methane admixture *Low Temp. Phys.* **26** 762–6

[13] Asheghi M, Kurabayashi K, Kasnavi R and Goodson K E 2002 Thermal conduction in doped single-crystal silicon films *J. Appl. Phys.* **91** 5079–88

[14] Song D and Chen G 2004 Thermal conductivity of periodic microporous silicon films *Appl. Phys. Lett.* **84** 687–9

[15] Stillinger F H and Weber T A 1985 Computer simulation of local order in condensed phases of silicon *Phys. Rev.* B **31** 5262–71

[16] Lukes J R, Li D Y, Liang X G and Tien C L 2000 Molecular dynamics study of solid thin-film thermal conductivity *J. Heat Trans.* **122** 536–43

[17] Volz S G and Chen G 2000 Molecular-dynamics simulation of thermal conductivity of silicon crystals *Phys. Rev.* B **61** 2651–6

[18] Volz S G and Chen G 1999 Molecular dynamics simulation of thermal conductivity of silicon nanowires *Appl. Phys. Lett.* **75** 2056–8

[19] Volz S G, Saulnier J-B, Chen G and Beauchamp P 2000 Molecular dynamics of heat transfer in Si/Ge superlattices *High Temp.—High Pressures* **32** 709–14

[20] Wang X, Huang Z, Wang T, Tang Y W and Zeng X C 2008 Structure and thermophysical properties of single-wall Si nanotubes *Phys. B: Condens. Matter* **403** 2021–8

[21] Maruyama S 2002 A molecular dynamics simulation of heat conduction in finite length SWNTs *Phys. B: Condens. Matter* **323** 193–5

[22] Che J, Cagin T, Deng W and William A G III 2000 Thermal conductivity of diamond and related materials from

molecular dynamics simulations *J. Chem. Phys.* **113** 6888–900
[23] Kitashima T, Kakimoto K and Ozoe H 2003 Molecular dynamics analysis of diffusion of point defects in GaAs *J. Electrochem. Soc.* **150** 198–202
[24] Abramson A R, Tien C-L and Majumdar A 2002 Interface and strain effects on the thermal conductivity of heterostructures: a molecular dynamics study *J. Heat Trans.* **124** 963–70
[25] Schiøtz J, Di Tolla F D and Jacobsen K W 1998 Softening of nanocrystalline metals at very small grain sizes *Nature* **391** 561–3
[26] Wang D, Wang W, Chen S, Huang J, Ren Z, Lee H, Chen G, Tang M, Dresselhaus M S, Gogna P, Fleurial J-P and Klotz B 2006 Characterization and thermoelectric properties of Si–Ge nanocomposite *APS March Meeting (Baltimore, MD, USA, 13 March 2006)*
[27] Qiao R and He P 2007 Simulation of heat conduction in nanocomposite using energy-conserving dissipative particle dynamics *Mol. Simul.* **33** 677–83
[28] Volz S G, Saulnier J B, Chen G and Beauchamp P 2000 Computation of thermal conductivity of Si/Ge superlattices by molecular dynamics techniques *Microelectron. J.* **31** 815–9
[29] Ikeshoji T and Hafskjold B 1994 Non-equilibrium molecular dynamics calculation of heat conduction in liquid and through liquid–gas interface *Mol. Phys.* **81** 251–61
[30] Maiti A, Mahan G D and Pantelides S T 1997 Dynamical simulations of nonequilibrium processes–heat flow and the Kapitza resistance across grain boundaries *Solid State Commun.* **102** 517–21
[31] Evans D J and Morris G P 1983 Nonequilibrium molecular-dynamics simulation of Couette flow in two-dimensional fluids *Phys. Rev. Lett.* **51** 1776–9
[32] Ryckaert P, Bellemans A, Ciccotti G and Paolini G V 1989 Evaluation of transport coefficients of simple fluids by molecular dynamics: comparison of Green–Kubo and nonequilibrium approaches for shear viscosity *Phys. Rev.* A **39** 259–67
[33] Gillan M J 1987 A simulation model for hydrogen in palladium: II. Mobility and thermotransport *J. Phys. C: Solid State Phys.* **20** 521–38
[34] Miller-Plathe F 1997 A simple nonequilibrium molecular dynamics method for calculating the thermal conductivity *J. Chem. Phys.* **106** 6082–5
[35] Jund P and Jullien R 1999 Molecular-dynamics calculation of the thermal conductivity of vitreous silica *Phys. Rev.* B **59** 13707–11
[36] Ding K and Andersen H C 1986 Molecular-dynamics simulation of amorphous germanium *Phys. Rev.* B **34** 6987–91
[37] Berger L I 2007 *CRC Handbook of Chemistry and Physics* ed D R Lide (Boca Raton, FL: Taylor and Francis)
[38] Kotake S and Wakuri S 1994 Molecular dynamics study of heat conduction in solid materials *JSME Int. J. Ser. B—Fluids Thermal Eng.* **37** 103–8
[39] Swope W C, Andersen H C, Berens P H and Wilson K R 1982 A computer simulation method for the calculation of equilibrium constants for the formation of physical clusters of molecules: application to small water clusters *J. Chem. Phys.* **76** 637–49
[40] Kapitza P L 1941 *J. Phys. (Moscow)* **4** 181
[41] Swartz E T and Pohl R O 1989 Thermal boundary resistance *Rev. Mod. Phys.* **61** 605–68
[42] Dresselhaus M S, Chen G, Tang M, Yang R, Lee H, Wang D, Ren Z, Fleurial J-P and Gogna P 2007 New directions for low-dimensional thermoelectric materials *Adv. Mater.* **19** 1043–53
[43] Lee S-M, Cahill D G and Venkatasubramanian R 1997 Thermal conductivity of Si–Ge superlattices *Appl. Phys. Lett.* **70** 2957–9
[44] Liu W L, Borca-Tasciuc T, Chen G, Liu J L and Wang K L 2001 Anisotropic thermal conductivity of Ge quantum-dot and symmetrically strained Si/Ge superlattices *J. Nanosci. Nanotechnol.* **1** 39–42
[45] Guo Z Y, Cao B Y, Zhu H Y and Zhang Q G 2007 State equation of phonon gas and conservation equations for phonon gas motion *Acta Phys. Sin.* **56** 3306–11
[46] Lee H 2005 Experimental study of thermal conductivity reduction of silicon–germanium nanocomposite for thermoelectric application *Massachusetts Institute of Technology. Department of Mechanical Engineering* (Boston, USA: Massachusetts Institute of Technology)